

# Integrated Antennas on MnM Interposer for the 60 GHz Band

J. E. G. Lé<sup>1</sup> , M. Ouvrier-Bufferet<sup>1</sup> , L. G. Gomes<sup>1</sup> , R. A. Penchel<sup>2</sup> , A. L. C. Serrano<sup>1</sup> ,  
G. P. Rehder<sup>1</sup> 

<sup>1</sup> Electronic Systems Department - LME, University of São Paulo - USP, São Paulo, Brazil, [joao.le@usp.br](mailto:joao.le@usp.br), [mathilde.ouvrier-bufferet@univ-grenoble-alpes.fr](mailto:mathilde.ouvrier-bufferet@univ-grenoble-alpes.fr), [leonardo.gomes@usp.br](mailto:leonardo.gomes@usp.br), [aserrano@usp.br](mailto:aserrano@usp.br), [gprehder@usp.br](mailto:gprehder@usp.br)

<sup>2</sup> São Paulo State University - Unesp, São João da Boa Vista, Brazil, [rafael.penchel@unesp.br](mailto:rafael.penchel@unesp.br)

**Abstract—** In this article, antennas for the 60 GHz ISM band designed to be integrated to a new high-frequency, low-cost interposer technology called Membrane-nanowire-Membrane (MnM) are discussed, manufactured, and measured. Also, an antenna characterization system under development at the Microelectronic Laboratory (LME-USP) is introduced, showing promising results for the deployment of mmW systems.

**Index Terms—** 3D integration, interposer, patch, quasi-yagi, antenna characterization system

## I. INTRODUCTION

The 60 GHz ISM band and its abundance of spectrum represent a great opportunity, not yet well explored, for ultra-high speed and short-range wireless communications. The challenges for its commercial use are different from that of consumer technologies below 6 GHz [1,2], which may influence the slow deployment. The first obstacle to large-scale exploitation is the high free-space path loss that the signal is subjected to and the great sensitivity to blockage. The radio coverage at 60 GHz requests higher density of base stations compared to communication technologies at lower frequencies. This means a higher infrastructure cost. High-gain antenna array with beamforming can be used to increase the cell coverage radius and, consequently, decrease antenna density. Also, low-cost approaches based on novel materials can be an answer to the widespread of systems in these frequency ranges.

The difficulty of integrating components on the same chip to form high frequency circuits is the second obstacle in using this band. At lower frequencies, it is feasible to insert the transceiver close to the central processing unit and route the signal to an antenna through cables or printed transmission lines. This antenna, in turn, will be in a place where its radiation pattern is best used. As the operating frequency increases, the antenna should be closer to the transceiver, to reduce the signal degradation. One of the alternatives would be to manufacture all components on the same substrate, in a monolithic Antenna-on-Chip (AoC) approach; however, different components take advantage of different substrates and the cost to integrate large passive circuits in advance CMOS/BiCMOS technologies for millimeter waves (mmW) can be prohibitive for consumer applications. Further, the high permittivity and low resistivity make silicon a bad choice in terms of irradiation efficiency [3]. As an example, [4]

achieved 38% efficiency by integrating the AoC into a PCB in order to increase the effective height of the substrate.

Another approach is to use a more suitable substrate for the antenna design. Many techniques have been proposed [5]-[7] using different substrates to obtain antennas with high gain and bandwidth to meet the necessary characteristics for the exploitation of these frequencies. However, antennas are only part of the system and its integration should be carefully considered.

The use of the Metallic-nanowire-Membrane (MnM) dielectric as an interposer and/or as a substrate is proposed for these technical-commercial dilemmas [8]-[16]. The use of an interposer has the purpose of creating a circuit with a 3D structure in order to (i) maximize the use of the area, which results in smaller circuits; (ii) decrease the distance between the components, decreasing the signal path losses; (iii) facilitating the integration of components of different technologies and characteristics: CMOS and power circuits, microstrip lines and antennas can be grouped in a common mechanical object.

In this paper, a brief review of the MnM technology, presenting its benefits as an interposer is shown in section II. Different approaches for the fabrication of antennas on the interposer or to be connected to it (on a different substrate), are proposed for the 60 GHz ISM band. Some of these antenna designs using MnM and Liquid Crystal Polymer dielectric (LCP, Rogers 3850HT Ultralam) are presented in section III. In section IV, the authors present the millimeter wave antenna characterization system under development. Finally, a conclusion is presented in section V.

## II. MNM INTERPOSER

A good interposer for mmW applications must be able to interconnect components manufactured in different substrates/technologies, and redistribute the signals accordingly. This can only be achieved if it is possible to (i) build through-substrate vias (TSVs) with very low losses for vertical integration and ground connections; and (ii) create high quality transmission lines for horizontal integration, which will also serve as building blocks for high performance circuits on the interposer.

Several very promising results were obtained with the MnM interposer that allows the design of transmission lines with high and low characteristic impedances (from 10  $\Omega$  to 140  $\Omega$ ) [8], Through Substrate Vias (TSVs) [9], 3D inductors [10], Substrate Integrated Waveguides (SIW) [11,12], among others. Fig. 1 illustrates some of the results obtained in the MnM interposer.

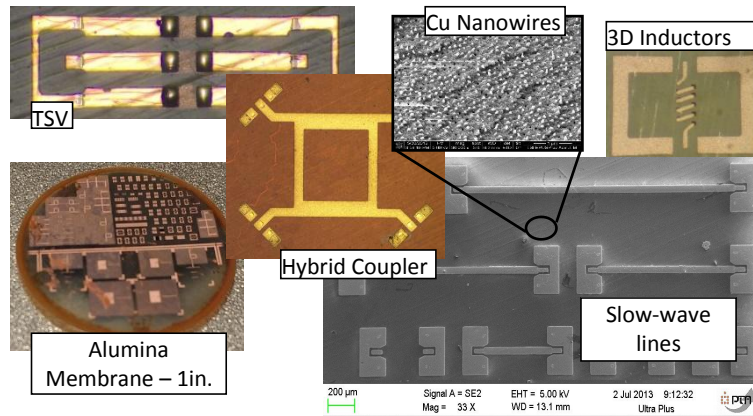


Fig. 1. MnM interposer devices: slow-wave microstrip lines, hybrid couplers, 3D inductors, TSVs and others.

The MnM platform is based on a nanoporous alumina substrate that has numerous benefits. Alumina is an excellent insulator with low loss at high frequencies. Nanoporous alumina can be obtained by electrochemical oxidation of aluminum under specific anodizing voltages and the process can be easily scaled, as demonstrated by the manufacturer (Inredox), with its large area membranes reaching  $45 \times 28 \text{ cm}^2$ .

The existence of nanopores is intrinsic to the manufacture of membranes and is advantageous for several reasons. The nanopores can be easily filled with metal by electrodeposition and form a bundle of nanowires that connect the two surfaces of the substrate in a simple manufacturing process, forming TSVs with state-of-the-art performance up to 110 GHz [13]. Further, the nanowires can be used to achieve slow wave effect in microstrip based-transmission lines, as presented in [14], [15], leading to a miniaturization of the wavelength-based devices.

To integrate active devices on the MnM interposer, an experimental low cost, in-house, flip-chip interconnection fabrication process based on copper pillars is under development with initial results presented in [16].

Several devices in mmW systems can be developed directly over the MnM interposer using a simple and low-cost fabrication process and, subsequently, integrated with both active and passive devices fabricated in CMOS and other technologies by any interconnection solution. That makes this platform a complete and possibly economical solution to be used in the transition of the communications market to the bands above 6 GHz. Fig. 2 shows a general idea of the possible integration solution with the MnM interposer for a transceiver module with beam-steering. In this example, a slot coupled with air cavity antenna is used.

### III. ANTENNAS ON INTERPOSER

In addition to a high gain, an imperative feature of antennas for systems operating at the 60 GHz ISM is having a wide bandwidth to cover all four channels (57-66 GHz). The purpose of this section, however, is to discuss the simulation, fabrication and measure of well-known antennas suitable for integration into an interposer. For this, there are two alternatives: to fabricate it directly on the

interposer, or to fabricate it on a commonly used substrate and connect it to the interposer via flip-chip. The first alternative is hampered by the high relative dielectric constant ( $\epsilon_r = 6.7$ ) and the loss tangent ( $\tan\delta = 0.01 @ 60 \text{ GHz}$ ) of the MnM, which leads to a low gain in a conventional rectangular patch, as presented in Section III-A. A higher gain and bandwidth can be achieved using a quasi-Yagi antenna, as shown in Section III-B, but still not enough to cover this entire band.

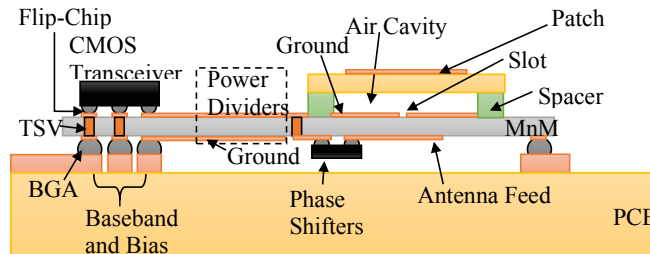


Fig. 2. Illustration of a mm-wave transceiver module with beam-steering on the MnM technology platform.

A suitable substrate for planar antennas is the Liquid Crystal Polymer (LCP, Rogers 3850HT Ultralam), that has a lower relative dielectric constant ( $\epsilon_r = 3.14$ ) and higher thickness ( $180 \mu\text{m}$ ). This substrate was also chosen for its low loss tangent at mm-waves ( $\tan\delta = 4 \times 10^{-3} @ 60 \text{ GHz}$  [17]). The realization of a patch antenna on LCP is presented in Section III-C. Despite the higher gain, the patch antenna is intrinsically narrow-banded.

All the measurements presented in this section were taken on a probe station with an MPI's Titan A67 probe ( $100\text{-}\mu\text{m}$  pitch) and the electromagnetic simulations were performed with ANSYS HFSS.

#### A. Patch Antenna on MnM

A rectangular patch antenna illustrated in Fig. 3 was realized on the MnM interposer. The patch was fed with a  $50\text{-}\Omega$  microstrip line,  $67\text{-}\mu\text{m}$  wide. A coplanar-to-microstrip transition was implemented at the RF pads using the TSVs of the MnM interposer. The antenna was fabricated on an anodic aluminum oxide membrane (AAO) from Inredox with nanopores with  $40 \text{ nm}$  in diameter. The fabrication process used was the same as described in [12] with electrodeposited copper layer of  $3 \mu\text{m}$ . The cross-section of the MnM technology is shown in Fig. 3 and the fabricated antenna is shown in the insert of Fig. 4.

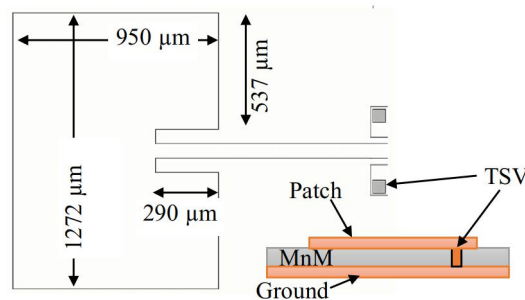


Fig. 3. Layout with dimensions of the rectangular patch antenna on the MnM interposer. MnM cross-section illustrating the technology used.

Fig. 4 presents a good agreement between the simulated and measured reflection coefficient of the rectangular patch antenna. A 1.14 GHz (1.9%) bandwidth (BW) was obtained considering a 10 dB return loss. The simulated maximum gain of this antenna is 2.7 dBi.

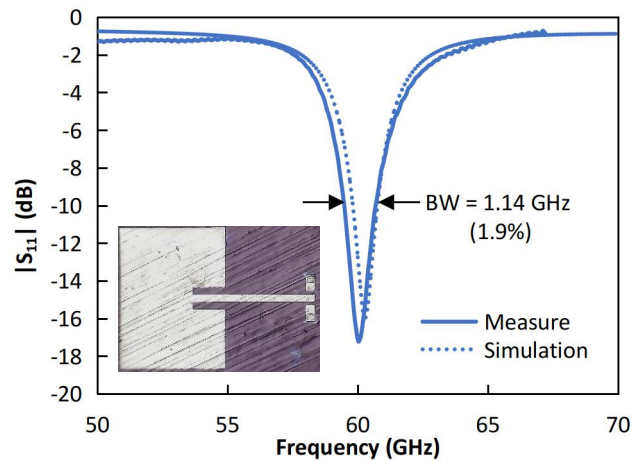


Fig. 4. Simulated and measured reflection coefficient of the rectangular patch antenna on the MnM interposer. Insert: Optical image of the fabricated antenna.

### B. Quasi-Yagi Antenna on MnM

The layout with dimensions of the quasi-Yagi antenna with a balun is presented in Fig. 5. The balun is used to convert a single-ended signal into a differential one. The insert of Fig. 6 shows the fabricated structure. The fabrication process used was the same as described in [13].

The measured and simulated frequency response of the quasi-Yagi antenna with balun is shown in Fig. 6. The 10 dB-bandwidth was measured to be 3 GHz (4.7%). The simulated gain of the quasi-Yagi antennas was 5.4 dBi.

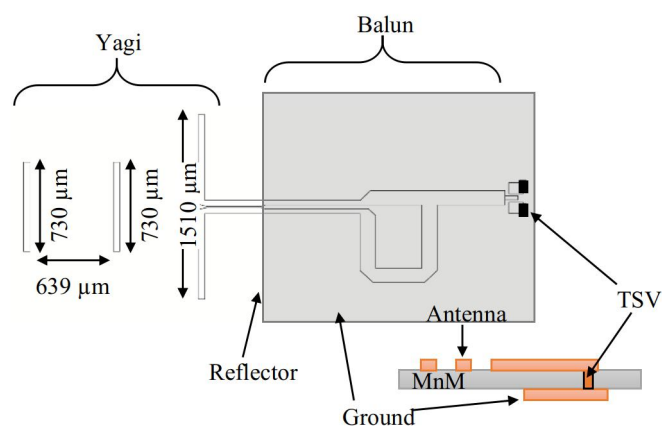


Fig. 5. Layout with dimensions of the quasi-yagi antenna on the MnM interposer. MnM cross-section illustrating the technology used.

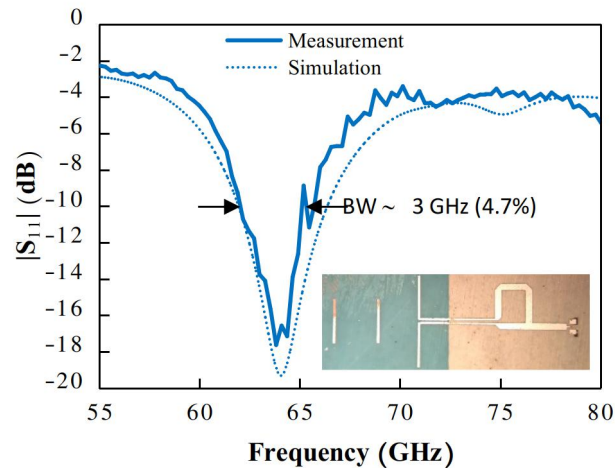


Fig. 6. Simulation and measurement of the Quasi-Yagi antenna on MnM with feeding balun. Insert: Optical image of the fabricated antenna.

### C. Patch Antenna on LCP

The layout with dimensions of the rectangular patch antenna is presented in Fig. 7. The patch was fed with a 50-Ω microstrip line, 95-μm wide. This antenna was conceived to be used at the output of a Analog Devices HMC6300 transmitter. The 50-Ω CPW line used to connect the transmitter to the antenna also couples its grounds to the patch and microstrip ground plane.

Because of the dimensions involved (50 μm gap for the CPW line) photolithography was used to pattern the antenna and feeding lines. First, the original copper film of the top surface of the LCP substrate was removed. Then, a thin (~20 nm) copper seed layer was sputtered on the top surface. The copper film was then thickened by electrodeposition up to 3 μm. The layout was pattern using photoresist (AZ1518) and the copper patterns was etched using a commercially available solution. An optical image of the fabricated structure is shown in the insert of Fig. 8.

The simulated and measured reflection coefficient of the rectangular patch fabricated on the LCP substrate is presented in Fig. 8. A small frequency shift from 60 GHz (design) to 60.5 GHz (measure) was observed. The manufacturer of the LCP substrate specifies its relative dielectric constant as 3.14 at 10 GHz. A dispersion in this value probably caused this shift. Furthermore, the obtained bandwidth was 1.2 GHz (2%) and the simulated gain was 7 dBi.

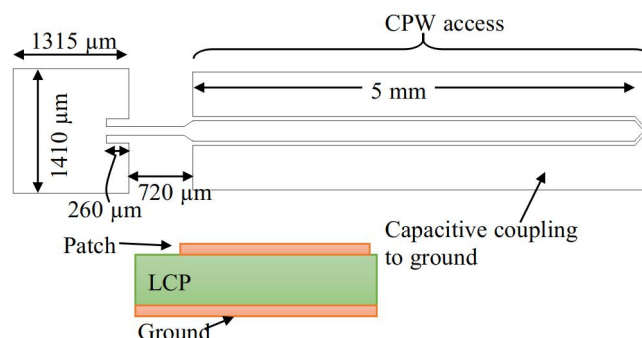


Fig. 7. Layout with dimensions of the rectangular patch antenna on LCP and technology cross-section.

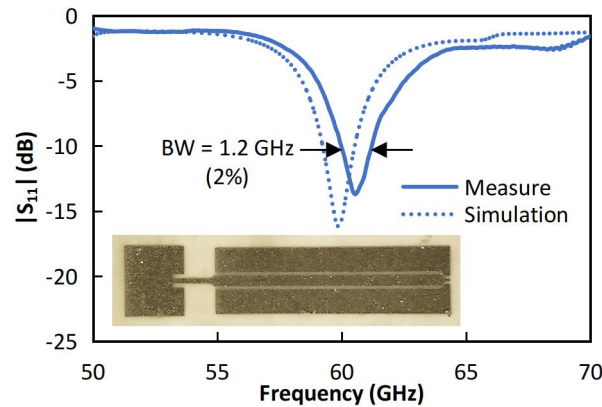


Fig. 8. Simulated and measured reflection coefficient of the rectangular patch antenna on LCP. Insert: Optical image of the fabricated antenna.

#### IV. MILLIMETER-WAVE MEASUREMENT SYSTEM

The mm-wave antenna characterization system under development at our laboratory is shown in Fig. 9. In this system, a reference horn antenna (50-70 GHz) is rotated around the fixed Antenna-Under-Test (AUT) using two stepper motors. The reference antenna is connected to a 4x frequency multiplier and the signal (12.5-17.5 GHz) is provided by the VNA (N5227B – Keysight). The AUT is connected directly to the VNA for measurement. The control and acquisition software was realized in LabVIEW. In Fig. 12, the AUT was replaced by a horn antenna for system calibration.

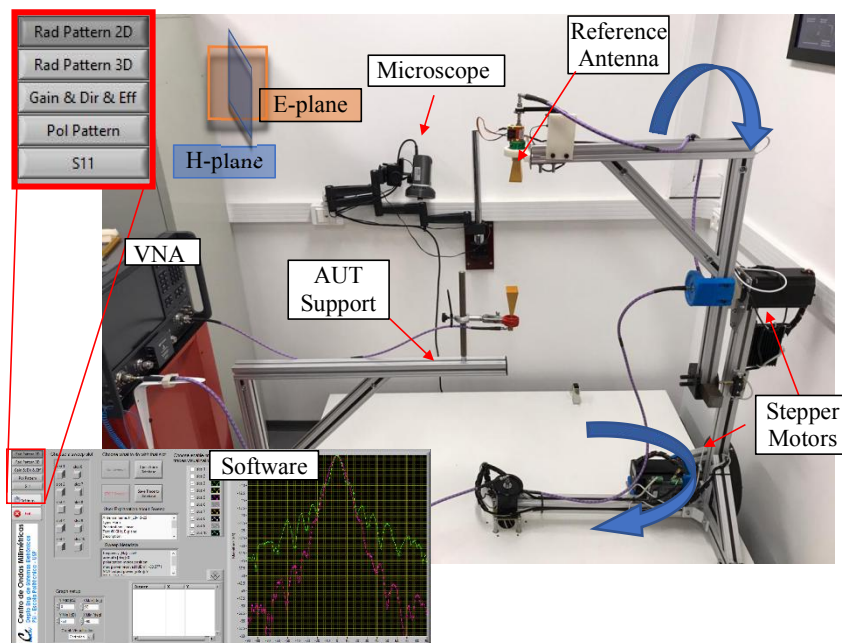


Fig. 9. Mm-Wave characterization system under development at the Laboratory of Microelectronics (mmW Center) of the University of São Paulo.

The AUT is supported by ROHACELL 51 IG foam with  $\epsilon_r=1.05$  and  $\tan\delta=0.0135$  at 26.5 GHz, as shown in Fig 10. A digital mobile microscope is used to place 67A-GSG-100 Picoprobe with an RVP-style body on the AUT. To prevent vibration and mechanical damage to the probes, the AUT support

is mechanically isolated from the rest of the building. A near complete sphere, limited only by the AUT support, can be measured with this system and all the main figures of merit from 50 GHz to 70 GHz can be obtained.

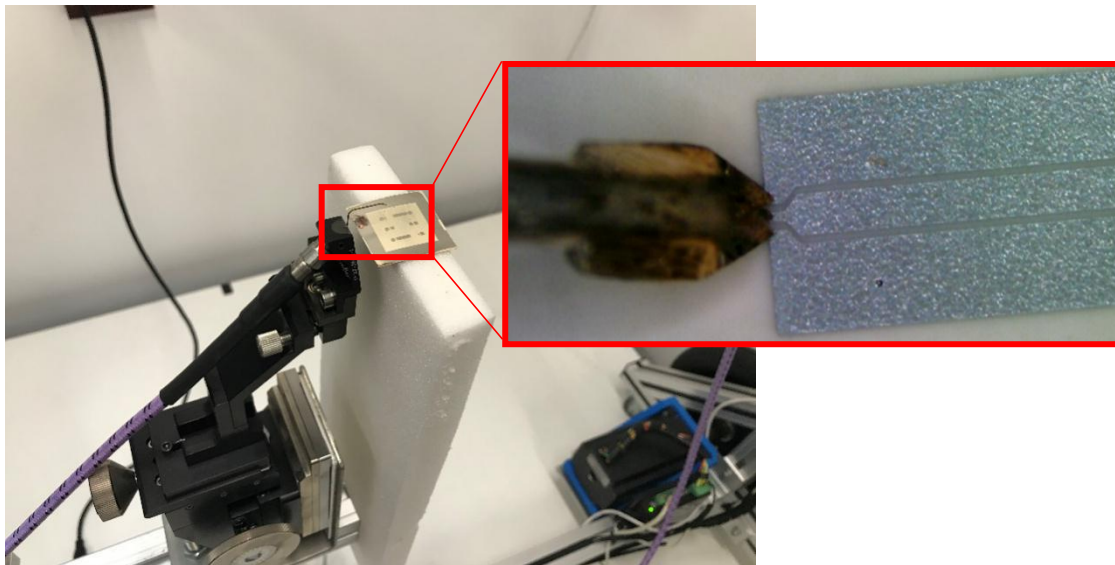


Fig. 10. AUT support and probe. In detail the connection of the probe with the patch antenna on LCP presented in Section III-C.

As stated, the antenna measurement system is still under development and absorbers should be added at strategic places to avoid unwanted reflections, but the results are promising. Preliminary measurement results of the patch antenna on LCP, presented in Section III-C, are presented here.

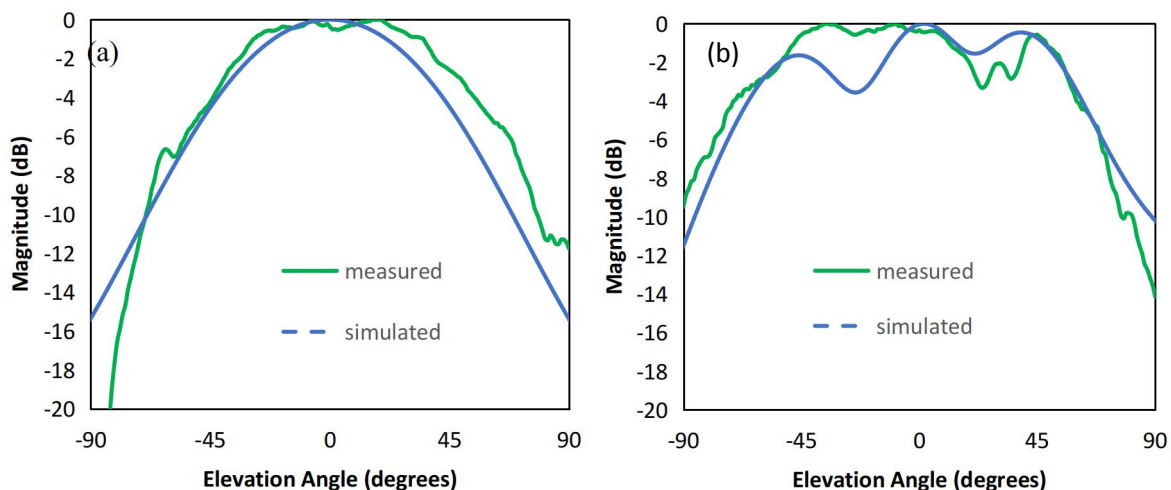


Fig. 11. Simulations and measurements of the Section III-C antenna. (a) H-plane and (b) the E-plane radiation patterns at 60.5 GHz.

The measured H-plane (Fig. 11(a)) and E-plane (Fig. 11(b)) radiation patterns at 60.5 GHz show good agreement between measurement and HFSS simulation. In Fig. 15 (a), the measurement of the H-plane polarization pattern is shown: for each elevation angle, the reference antenna is rotated between co and cross-polarization positions [18]. This result allows the calculation of the axial ratio at

any direction of the measured 2-D pattern simply by subtracting the maximum (co-polarization) and minimum (cross-polarization) magnitude values. The axial ratio of this antenna varies between 14.3 dB (25° elevation) and 5.4 dB (-50° elevation). Fig. 15 (b) presents the measured maximum gain; at 60.5 GHz, the measured gain was 7.06 dBi, similar to the simulated 7 dBi.

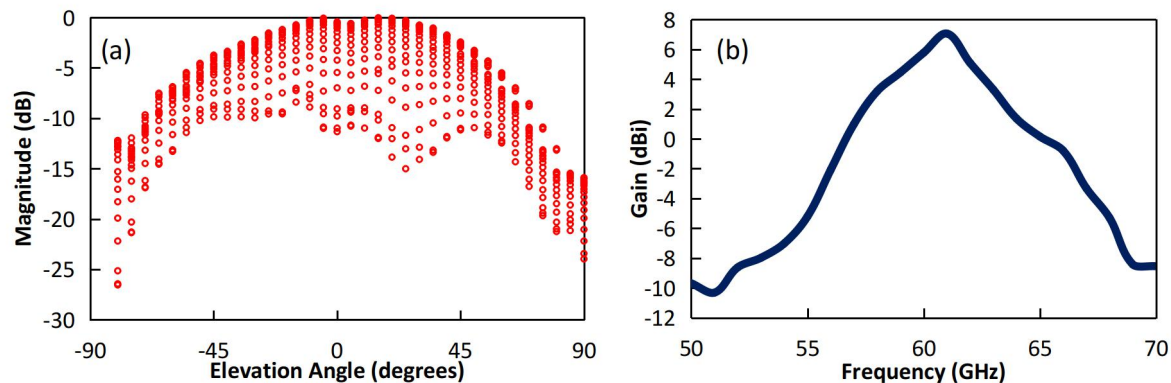


Fig. 15. Measurements of the Section III-C antenna. (a) The polarization pattern of H-plane at 60.5 GHz; in (d), the gain versus frequency.

## V. CONCLUSION

The MnM interposer that is being studied to be used in a 60 GHz ISM transceiver module was presented. Here, different possibilities for integrated antennas were tested: rectangular patch on the MnM interposer; quasi-yagi antenna with balun on the MnM interposer; rectangular patch on LCP substrate. There is a good agreement between the simulation and measurements of these basic antennas, which means that the group is ready to design more sophisticated antennas.

This work also presented the antenna characterization system under development at the Microelectronics Laboratory at the University of São Paulo, and its initial results.

## ACKNOWLEDGMENT

The authors would like to acknowledge the financial support of FAPESP with the acquisition of the multiuser VNA up to 110 GHz (EMU project 2016/25779-9) and CNPq (process 431200/18-1).

## REFERENCES

- [1] T. Yilmaz and O. B. Akan, "State-of-the-art and research challenges for consumer wireless communications at 60 GHz", *IEEE Trans. Consum. Electron.*, vol. 62, no. 3, 2016.
- [2] R.C. Daniels and R.W. Heath, "60 GHz wireless communications: emerging requirements and design recommendations", *IEEE Veh. Technol. Mag.*, vol. 2, no. 3, pp. 41-50, 2007.
- [3] Y. P. Zhang and D. Liu, "Antenna-on-Chip and Antenna-in-Package Solutions to Highly Integrated Millimeter-Wave Devices for Wireless Communications," in *IEEE Transactions on Antennas and Propagation*, vol. 57, no. 10, pp. 2830-2841, Oct. 2009.
- [4] M. K. Hedayati et al., "Challenges in On-Chip Antenna Design and Integration With RF Receiver Front-End Circuitry in Nanoscale CMOS for 5G Communication Systems," in *IEEE Access*, vol. 7, pp. 43190-43204, 2019.
- [5] T. H. Jang, Y. H. Han, J. Kim and C. S. Park, "60 GHz Wideband Low-Profile Circularly Polarized Patch Antenna With an Asymmetric Inset," in *IEEE Antennas and Wireless Propagation Letters*, vol. 19, no. 1, pp. 44-48, Jan. 2020.
- [6] A. Jaiswal, M. P. Abegaonkar and S. K. Koul, "Highly Efficient, Wideband Microstrip Patch Antenna With Recessed Ground at 60 GHz," in *IEEE Transactions on Antennas and Propagation*, vol. 67, no. 4, pp. 2280-2288, April 2019.
- [7] J. Zhu, Y. Yang, C. Chu, S. Li, S. Liao and Q. Xue, "60-GHz High Gain Planar Aperture Antenna Using Low-Temperature Cofired Ceramics (LTCC) Technology," *2019 IEEE MTT-S International Wireless Symposium (IWS)*, Guangzhou, China, pp. 1-3, 2019.
- [8] M. V. Pelegrini et al., "Interposer based on metallic-nanowire-membrane (MnM) for mm-wave applications," *11th European Microwave Integrated Circuits Conference (EuMIC)*, London, 2016, pp. 532-535, 2016.

- [9] J. M. Pinheiro, M. V. Pelegrini, L. Amorese, P. Ferrari, G. P. Rehder, and A. L. C. Serrano, "Nanowire-based through substrate via for millimeter-wave frequencies," in *IEEE MTT-S Int. Microw. Symp. Dig.*, San Francisco, CA, USA, pp. 1-4, May 2016.
- [10] A. L. C. Serrano et al., "3D inductors with nanowire through substrate vias," *2017 IEEE MTT-S International Microwave Symposium (IMS)*, Honolulu, HI, pp. 1641-1644, 2017.
- [11] J. Corsi, G. P. Rehder, L. G. Gomes, M. Bertrand, A. L. C. Serrano, E. Pistono, P. Ferrari, Partially-Air-Filled Slow-Wave Substrate Integrated Waveguide in Metallic Nanowire Membrane Technology, In: *2020 IEEE/MTTS IMS 2020*.
- [12] M. Bertrand, et al. "Integrated Waveguides in Nanoporous Alumina Membrane for Millimeter-Wave Interposer," *IEEE Microwave and Wireless Components Letters*, vol. 29, no. 2, pp. 83-85, 2019.
- [13] J. M. Pinheiro et al., "110-GHz Through-Substrate-Via Transition Based on Copper Nanowires in Alumina Membrane," in *IEEE Transactions on Microwave Theory and Techniques*, vol. 66, no. 2, pp. 784-790, Feb. 2018.
- [14] A. L. C. Serrano et al., "Slow-wave microstrip line on nanowire-based alumina membrane," *2014 IEEE MTT-S International Microwave Symposium (IMS2014)*, Tampa, FL, pp. 1-4, 2014.
- [15] A. L. C. Serrano et al., "Modeling and Characterization of Slow-Wave Microstrip Lines on Metallic-Nanowire- Filled-Membrane Substrate," in *IEEE Transactions on Microwave Theory and Techniques*, vol. 62, no. 12, pp. 3249-3254, Dec. 2014.
- [16] F. S. Bedoya, A. L. C. Serrano and G. P. Rehder, "Mm-wave flip-chip fabrication process for MnM-based interposer interconnection," *2017 32nd Symposium on Microelectronics Technology and Devices (SBMicro)*, Fortaleza, pp. 1-4, 2017.
- [17] D. C. Thompson, O. Tantot, H. Jallageas, G. E. Ponchak, M. M. Tentzeris and J. Papapolymerou, "Characterization of liquid crystal polymer (LCP) material and transmission lines on LCP substrates from 30 to 110 GHz," in *IEEE Transactions on Microwave Theory and Techniques*, vol. 52, no. 4, pp. 1343-1352, April 2004.
- [18] C. A. Balanis, "Antenna Measurements," in *Modern Antenna Handbook*, Wiley, pp.977-1033, 2008.

## ERRATA

**On page 184, the sixth author's name has been incorrectly given in the original version:**

K. G. P. Rehder

**The correct name is:**

G. P. Rehder